



1           **Evaporative fractionation of H<sub>2</sub><sup>18</sup>O in the polar ocean and the**  
2           **invisibility of large changes of ice volume and sea level in the Saalian**  
3                           **δ<sup>18</sup>O proxy records**  
4                           Robert G. Johnson  
5                           [glenjay@bitstream.net](mailto:glenjay@bitstream.net)  
6                   Department of Earth Sciences  
7                   University of Minnesota  
8                   310 Pillsbury Drive SE  
9                   Minneapolis MN 55455-0231  
10  
11



1

2 **Abstract**

3 The oxygen isotope ratio,  $\delta^{18}\text{O}$ , as measured in skeletons of oceanic foraminifera,  
4 is a proxy for changes in world glacial ice volume and sea level and is of fundamental  
5 importance in the study of past climate change. However, in the Late Saalian glaciation  
6 the  $\delta^{18}\text{O}$  proxy reflects neither a large increase in glacial ice volume from 155 ka-142 ka  
7 nor the subsequent major deglaciation from 142 ka-136.5 ka in which sea level rose from  
8 about -140 m to +4 m at the end of the Drenthe sub stage. This deglaciation was caused  
9 by a large reduction in the ice sheet moisture supply caused by storm path diversion  
10 associated with the loss of thermohaline circulation and the capping of the high latitude  
11 North Atlantic with melt water that passed through the Mediterranean Sea from the  
12 overflow of a giant ice-blocked Siberian lake. The  $\delta^{18}\text{O}$  proxy also fails to record the  
13 subsequent ice volume buildup of the Warthe substage in which sea level fell about 80 m.  
14 The explanation for the invisibility involves the fractionation and sequestration of large  
15 amounts of  $\text{H}_2^{18}\text{O}$  in the effectively isolated and sea-ice-free deep polar ocean. The  
16 sequestration and subsequent release of polar water, enriched in  $\text{H}_2^{18}\text{O}$ , distorted the  
17 fractionation record in the world ocean and destroyed the accuracy of the  $\delta^{18}\text{O}$  proxy. The  
18 proposed physical consequences of the ice-free polar ocean also include a sea-ice-free  
19 Labrador Sea and Baffin Bay and an oceanic circulation mode that drove the Drenthe sub  
20 stage glaciation to its maximum extent in Eurasia. The initial cause for the anomalous  
21 effects in the  $\delta^{18}\text{O}$  record was the known ice-flow blockage of all the Siberian rivers that  
22 discharge into the polar ocean west of the Lena River. Without adequate stratification by  
23 inflowing fresh river water, sea ice was unable to freeze on the deep polar ocean and the  
24 fractionation and the physical changes in the polar ocean that are described here  
25 followed.

26

27 **Introduction**

28 Arkhipov et al, (1995) published a summary of glacial drainage conditions at the  
29 maxima of the Weichselian and Saalian glaciations that occurred in the last two ice age  
30 cycles beginning about 160 ka (ka = thousands of years before present). This paper was  
31 of fundamental interest because it also outlined a concept of major deglaciation caused by  
32 the reduction of precipitation on the ice sheets by means of atmospheric circulation  
33 changes associated with changes in thermohaline oceanic circulation. The deglaciation of  
34 the Drenthe sub stage of the Saalian glaciation was the cited example. However, this  
35 concept was contrary to the popular Milankovitch hypothesis (Milankovitch, 1930;  
36 Hodell, 2016) of direct control of glacial changes by Northern Hemisphere orbital high  
37 latitude summer insolation, a concept that has been supported by frequency correlations  
38 in the  $\delta^{18}\text{O}$  records (Hays et al., 1976). Furthermore, there was no support for a Drenthe  
39 substage deglaciation in the oceanic oxygen isotope ratio data. This contrasts with the  
40 deglaciation of the following Warthe substage that is easily identified with Termination 2  
41 in the  $\delta^{18}\text{O}$  records.

42

43 Since 1995 the published results of the analysis of sea stands at locations having  
44 varying uplift rates on Barbados (Johnson, 2001) have established a sea level slightly  
45 above present at 136.5 ka that is identified with the Drenthe deglaciation. In addition the  
46 causative aspect of the simple Milankovitch hypothesis has been weakened (Wunsch,  
2004) who showed statistically that the variance in the  $\delta^{18}\text{O}$  sea level proxy is largely



1 random over long time intervals. In the data discussed in this paper, the observed sea  
2 level rise that was caused by the deglaciation of the Drenthe substage during an insolation  
3 minimum, and the sea level fall due to the Warthe glacial ice accumulation under steadily  
4 rising Northern summer insolation are both in conflict with the Milankovitch hypothesis,  
5 and are invisible in the oceanic  $\delta^{18}\text{O}$  record. This invisibility is a consequence of  
6 fractionation in the ice-free polar ocean. However, to grasp the complete significance of  
7 the fractionation it is necessary to examine its cause, and the associated effects of the  
8 cause on the strength and location of deep-water formation, that is, on the thermohaline  
9 circulation in the northern North Atlantic. Therefore in this paper Sects. 1-4 describe the  
10 physical principles and evidence for events that led to the ice-free polar ocean and the  
11 fractionation. Sects. 5-7 outline the sequence of fractionation events and others that  
12 resulted from the ice-free polar ocean.

13

## 14 **1 Defining the invisibility problem and the related importance of storm path** 15 **location**

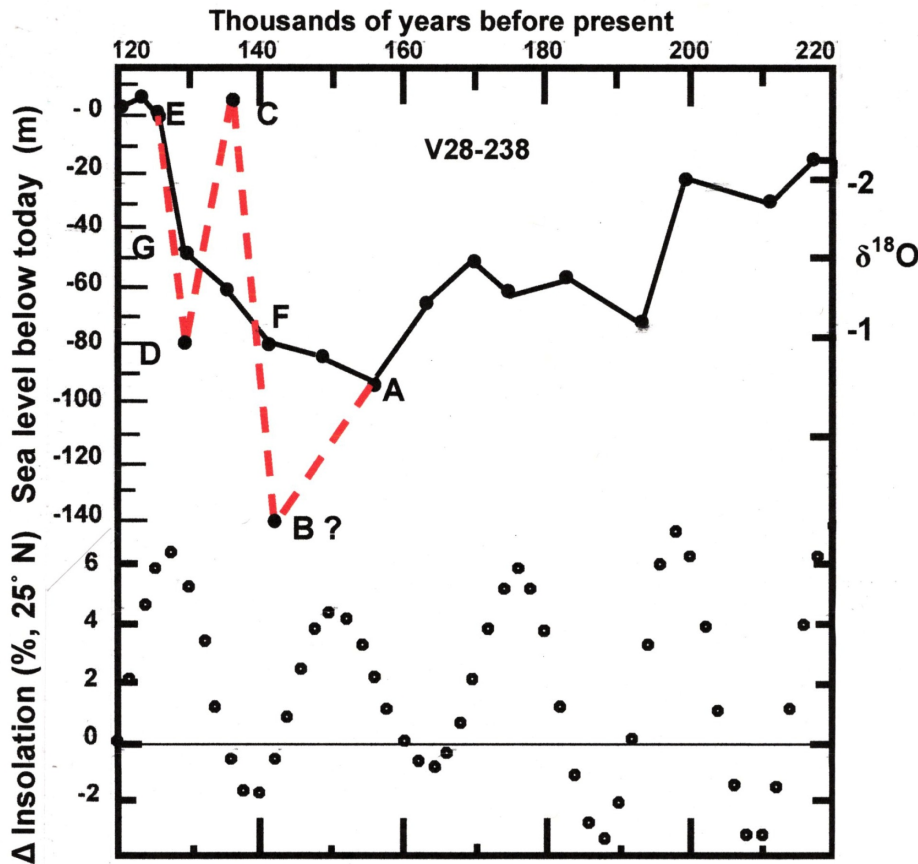
### 16 **1.1 The $\delta^{18}\text{O}$ oxygen isotope ratio proxy for world sea level and conflicting** 17 **coral reef data**

18 The riddle of the cyclic Plio-Pleistocene ice ages with their wide swings of world sea  
19 level and ice volume has been largely defined by  $\delta^{18}\text{O}$ , the algebraic form of the oxygen  
20 isotope ratio proxy for changes in glacial ice volume and world sea level. As measured in  
21 continuously deposited deep-sea sediments that are rich in foraminifera, the  $\delta^{18}\text{O}$  isotope  
22 ratio has long been a useful tool in the investigations of paleoclimates. The changes in the  
23 ratio occur because the heavier molecule of ocean water,  $\text{H}_2^{18}\text{O}$ , evaporates much more  
24 slowly than  $\text{H}_2^{16}\text{O}$  thus fractionating and enriching  $\text{H}_2^{18}\text{O}$  in the world ocean when the  
25 depleted precipitation is locked into glacial ice. Ideally, the measured  $\delta^{18}\text{O}$  is a good proxy  
26 for changes in glacial ice volume and the resulting variations in world sea level, and is  
27 particularly relevant in attempts to determine the cause of ice age climate variations.

28 Wunsch (2004) has shown by extensive analysis that most of the  $\delta^{18}\text{O}$  proxy  
29 variance is not explained by high latitude insolation changes, and is more likely to have  
30 been caused by internal variations within Earth's climate system. Therefore despite the  
31 correlations (Hays et al., 1976), the Milankovitch concept of orbital control of high latitude  
32 Northern summer insolation can not be a significant cause of the glacial climate variations.  
33 To identify the dominant causes it is important to find out how the internal factors act with  
34 the external orbital effects to cause the observed  $\delta^{18}\text{O}$  proxy changes. This paper is an effort  
35 to contribute to that goal by explaining the conflict between an inferred low sea level found  
36 in the  $\delta^{18}\text{O}$  proxy records of deep-sea cores during the Drenthe substage of the Saalian  
37 glaciation (Fig. 1), and the physical evidence for a simultaneous paleo sea stand at 4 m  
38 above present at 136.5 ka. A related conflict occurs in the subsequent Warthe substage of  
39 the Saalian. The Saalian name is used here for the entire Eurasian glaciation of that time.  
40 The explanation for this conflict involves the blockage of Siberian rivers by glacial ice flow,  
41 a quite different ice-free polar ocean circulation, and the fractionation of  $\text{H}_2^{18}\text{O}$  and its  
42 sequestration in the deep polar ocean. The conflict between observed sea level change and  
43 the isotope ratio proxy ended after orbitally controlled summer insolation (Berger, 1978)  
44 generated very strong African monsoons (Rossignol-Strick, 1983; Rossignol-Strick et al.,  
45 1998) that capped the northern North Atlantic with lower salinity Mediterranean outflow  
46 and melt water and started the Warthe deglaciation of Termination 2.



1



2

3 **Figure 1** Oxygen isotope ratio record for a benthic species in core V28-238  
4 during the Saalian glaciation from 200 ka to 126 ka. Dashed red line is the proposed  
5 true world sea level after the blockage of Siberian rivers by glacial ice began about  
6 156 ka. Dotted cycles are % deviation of the Northern caloric summer insolation  
7 average at 25° N from the modern 1950 value of 918 langley day<sup>-1</sup> ( $3.84 \times 10^7 \text{ j m}^{-2} \text{ day}^{-1}$ ).  
8  $\delta^{18}\text{O}$  values from Shackleton and Opdyke (1973). Insolation from tables supplied  
9 by Berger (1978).

10

11 The Drenthe high sea stand anomaly has been known for some time from prominent  
12 fossil coral reefs of controversial age on the rapidly uplifted Huon Peninsula in New Guinea  
13 (Chappell, 1974). The same sea stand is found on the more slowly uplifted island of Barbados  
14 where most of the resulting reef structure, except for the wave-cut erosion at the brief  
15 maximum sea stand itself, is buried beneath the subsequent coral deposits of the last  
16 interglacial. This sea stand on Barbados has been dated by a differential uplift method  
17 (Johnson, 2001) that is grounded on reliable thorium-uranium dates for Australian corals that  
18 grew at the end of the last interglacial (Stirling et al., 1995) and which, after a small correction  
19 (Johnson, 2015a) yields a sea level of +4m at 136.5 ka. This deglaciation occurred during an



1 interval of low Northern summer insolation, and it is diametrically opposed to the hypothesis  
2 (Milankovitch, 1930) of control of glaciation by orbital effects on Northern Hemisphere high  
3 latitude solar insolation

## 4 **1.2 Storm path variation: The importance of storm path location**

### 5 **1.2.1 A high Arctic example**

6 To interpret the complex data from Earth's climate system during the Saalian  
7 glaciation it is necessary to consider the critical conditions within the system that change  
8 precipitation rates on the world ice sheets. Although cold climate temperatures are necessary  
9 for the maintenance of an ice sheet, the moisture supply is equally important. The rate of  
10 growth or shrinkage of an ice sheet depends on the balance between loss of ice due to  
11 seasonal melting or discharge into the sea and the gain of ice due to storm precipitation.  
12 Without adequate moisture supplied by storms, ice sheets shrink. With a good supply they  
13 grow. On the matter of world glacial ice volume growth and shrinkage, the importance of the  
14 paths of storms that carry moisture from the ocean to the ice sheets cannot be overstated.  
15 Obvious examples are arid Peary Land on the northern tip of Greenland and much of  
16 Ellesmere Island to the west. The climate is quite cold in these regions, with Peary Land only  
17 800 km from the pole. Yet these areas are largely free of glacial ice because storms are  
18 infrequent and precipitation rates today are quite low. But the coasts are deeply indented by  
19 fiords, indicating that in times past large ice sheets, fed by frequent storms, occupied the  
20 land, see Sect. 5.3. Now the closest frequent storms are far away to the south. Today, with  
21 strong thermohaline circulation (THC) and resulting northward heat transport, storms are  
22 steered northeastward through the Greenland-Norwegian Sea basin by the temperature  
23 gradient between the cold Greenland ice sheet and the warmer water of the Greenland-  
24 Norwegian Sea, and much of their precipitation falls into the ocean. In most ice ages with a  
25 modest reduction of today's interglacial THC, the sea surface in the basin cools. Storm paths  
26 then shift southward and pass over Scandinavia, feeding the ice sheet there.

### 27 **1.2.2 A modern example: the Little Ice Age cycle**

28 As seen in the context of the 1500 yr deep ocean oscillation (Johnson, 2015b), the  
29 sea surface salinity (SSS) of the Greenland-Norwegian Sea basin plays a role in the THC,  
30 and the Little Ice Age can be explained by the effect of the varying basin salinity on the  
31 deep circulation and on the sea surface temperature (SST) gradients. The paths of storms  
32 tend to lie perpendicular to the strongest gradients. When the basin SSS is high, a greater  
33 amount of sinking deep-water feeds the large-scale THC. The sinking water is then  
34 replaced by a stronger North Atlantic Drift, the basin SST is warmer, and storms extend  
35 far northward in the Greenland-Norwegian Sea. When the basin SSS is lower, the THC is  
36 weaker, the basin SST is also lower, and the stronger gradient and storm paths lie to the  
37 south, with more storms extending over Scandinavia. The SSS would have been near a  
38 maximum a thousand years ago when populations were large in the cooler northern parts  
39 of the British Isles, and the pastoral Norse established colonies on southern Greenland.  
40 But as the basin salinity was reduced by the deep ocean oscillation, the THC became  
41 weaker, the climate cooled on Greenland and the British Isles, and those higher latitude  
42 areas were largely abandoned. Near the Little Ice Age extreme about the year 1750, as  
43 described by Lamb, wine grapes no longer grew in southern England and the winter sea  
44 ice in some years extended almost as far south as northern Scotland (Lamb, 1995).

45 In contrast, the salinity in the basin is today increasing because of the cyclic deep  
46 ocean oscillation, and also because of the effect of modern society's technical activities



1 on the Mediterranean Sea salinity. Excess atmospheric CO<sub>2</sub> warming should increase  
2 evaporation rates in the arid zones that include the Mediterranean Sea. The rising  
3 evaporation rates and the dams constructed for irrigation on nearly all the major rivers  
4 discharging into the Mediterranean are probably causing the measured increase in  
5 Mediterranean salinity and that of its outflow, which feeds significant saltier water  
6 northward into the Greenland-Norwegian Sea basin. Before these modern technical  
7 effects appeared, the cyclic salinity increase in the basin was already limiting the  
8 southward extent of the mid winter sea ice to the southern tip of Spitsbergen in most  
9 winters (Lamb, 1972). Now however, with technically enhanced salinity, the warmer  
10 southern water replacing the greater amount of sinking surface water in the THC keeps  
11 the mid winter sea ice limit well to the north of Spitsbergen's north coast, as shown by  
12 satellite images posted on the internet by the Technical University of Denmark in recent  
13 years. The lesson we get from the Little Ice Age's 1500 yr cycle is that the sea surface  
14 salinity in the Greenland-Norwegian sea basin determines the paths of the storms, and if  
15 the SSS becomes extremely low deep water would not form there and storm paths would  
16 be much farther to the south than society has seen in historic times.

### 17 **1.3 A long term orbital factor: orbitally-controlled African monsoons**

18 In the matter of shifting northern North Atlantic storm paths, African monsoons  
19 can play an indirect but decisive role. Strong monsoons occur when Earth in its eccentric  
20 orbit comes closest to the sun during Northern summer due to the 23,000 yr cyclic  
21 precession effect. Higher summer temperatures in the large land area of northern Africa  
22 relative to temperatures in the ocean areas and smaller African land area south of the  
23 equator then generate quite strong monsoons, which can extend northward over the  
24 Sahara and greatly increase Nile River flow (Rossignol-Strick, 1983; Rossignol-Strick et  
25 al., 1998). Strong monsoons therefore reduce the salinity of the Mediterranean Sea and its  
26 outflow at Gibraltar and the salinity of the higher latitudes where winter-cooled saline  
27 surface water sinks, thus driving the THC. The mixing time of the Mediterranean Sea is  
28 about 120 yrs as estimated from the exchange current flow (Bryden and Kinder, 1991)  
29 and the intervals of strong monsoons can last for ~4,000 yrs. Consequently the  
30 Mediterranean's reduced salinity and outflow closely tracks the occurrence of the strong  
31 monsoons. If not inhibited by a cold glacial climate extreme in northern Africa, the strong  
32 monsoons can reduce the THC, cool the high latitudes, and move the storm paths far to  
33 the south away from the Canadian and Scandinavian ice sheets giving them a dry glacial  
34 climate. On the other hand, warmer water in the sub polar North Atlantic adjacent to cold  
35 land tends to bring heavy precipitation over the land and cause ice sheet growth as  
36 reported by Ruddiman and McIntyre (1979). A somewhat different mechanism affecting  
37 Eurasian glaciation probably occurred due to sea-land temperature contrasts in western  
38 Europe and northwest Africa, as discussed in Sect. 4.2.

39 The orbital-monsoon mechanism is important, but like the hypothetical Milankovitch  
40 mechanism of direct control of glaciation by high latitude insolation, it can likewise be  
41 overcome by other effects within the climate system. An important example is framed in the  
42 following question: Why is decreasing insolation so often associated with glacial growth in  
43 the isotope ratio records, whereas the same level of increasing insolation seemingly causes  
44 deglaciation? Again the answer is found in the paths of storms governed by temperature  
45 gradients over the high latitude ocean. Weak and falling insolation at latitude 25° N does  
46 cause glacial ice volume to increase by weakening the monsoons, which then increases high-



1 latitude North Atlantic salinity and THC during already-established glaciation, and so  
2 indirectly steers storms over growing ice sheets. But at the same level of rising insolation  
3 massive Northern ice sheets are more likely to have been accumulated, and any factor that  
4 increases their melt water output may further decrease the high latitude salinity, cool the  
5 northern sea surface, and move the high latitude North Atlantic storm paths away from the ice  
6 sheets and far to the south, thus starving them of moisture. This is particularly true for the  
7 Canadian and Scandinavian ice sheets because their melt water is discharged into the areas of  
8 sinking THC water and this tends to reduce salinity and sinking rate and maintain colder sea  
9 surfaces. Other events also do so, including ice dam failures in Hudson Strait (Johnson and  
10 Lauritzen, 1995) and in the Baltic Sea outlet, and the Heinrich iceberg events (Heinrich,  
11 1988), that is, the “collapse” of the great Canadian ice sheet. In the  $\delta^{18}\text{O}$  records of the  
12 Pleistocene it is only when the large ice volumes are inferred at glacial extremes that major ice  
13 age terminations occur. It is in just such a context of the Saalian glacial extreme that the  
14 overflow of a giant ice-blocked lake in Siberia (Fig. 2) eliminated North Atlantic high latitude  
15 THC, and triggered a dry-climate deglaciation that brought the world ocean up to a sea level  
16 of +4 m with only a small change in the  $\delta^{18}\text{O}$  record (Johnson, 2001; Johnson, 2015a).

17

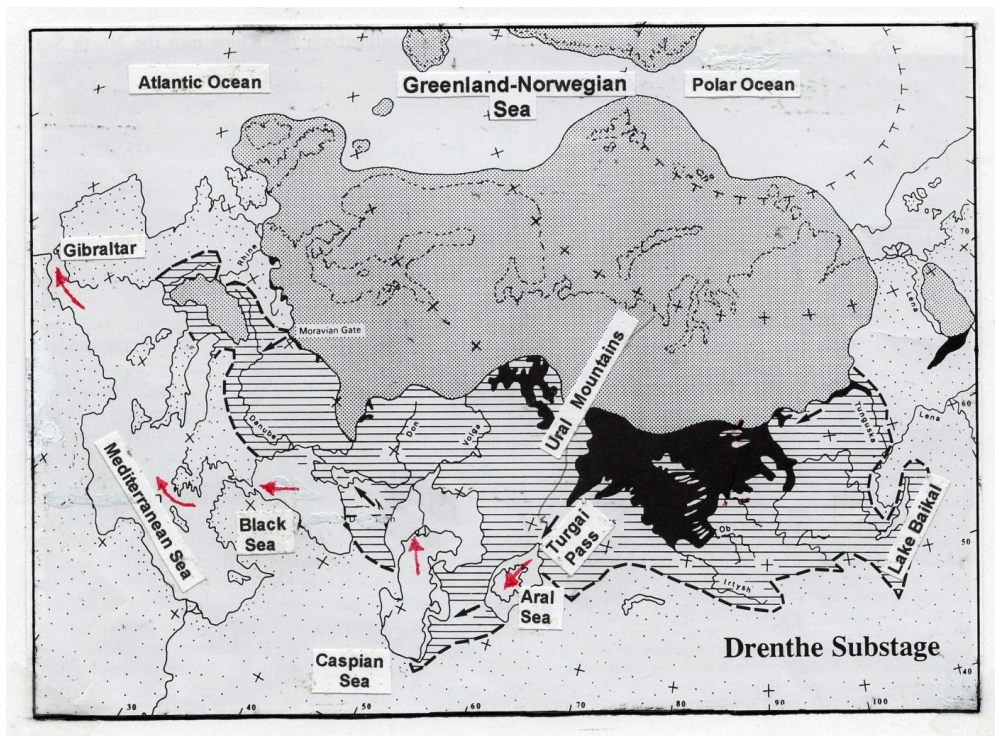
## 18 **2 Where the $\delta^{18}\text{O}$ proxy record failed: inferred Late Saalian ice volume and sea** 19 **level changes in the benthic sediment record of core V28-238**

20 Core V28-238 (Fig. 1) was recovered from a depth of 3120 m in the western Pacific  
21 where sedimentation rates are low and uniform (Shackleton and Opdyke, 1973). Benthic  
22 foraminifera living at that location and depth experienced a relatively constant temperature  
23 close to  $0^\circ\text{C}$ . Therefore the  $\delta^{18}\text{O}$  measured in their skeletons should provide a good record of  
24 ice volume and world sea level changes over time. This is approximately true because  $\delta^{18}\text{O}$   
25 values from that core and core V28-239 were used with calculated insolation variations  
26 (Berger, 1978) to obtain the first correct date of about 790 ka for earth’s last magnetic field  
27 reversal (Johnson, 1982). Extensive statistical analysis of the records of these two and many  
28 other cores has shown that the  $\delta^{18}\text{O}$  changes have the same principal frequencies as variations  
29 in orbital insolation that are caused by the precession effect, which determines the position of  
30 summer in the earth’s orbit, and by small changes in the tilt of the earth’s polar axis (Hays et  
31 al., 1976). Nevertheless, the core records are not free of proxy error, as in the V28-238 record  
32 of the Saalian glaciation discussed here. In this core a puzzling departure from the statistical  
33 expectation occurs at 175 ka when a somewhat lower (more positive)  $\delta^{18}\text{O}$  value is found  
34 instead of a negative peak consistent with higher insolation and stronger monsoons. At 150 ka  
35 there is no  $\delta^{18}\text{O}$  evidence for deglaciation despite an insolation peak (Berger, 1978) at  $25^\circ\text{N}$   
36 that is almost identical to the peak at 11 ka that is associated with the deglaciation of  
37 Termination 1 near the beginning of the Holocene. A third example is the focus of this paper,  
38 which is the difference between the observed and dated high sea stand at 136.5 ka (Johnson,  
39 2001; Johnson, 2015a) and the more positive values (lower on the page in conventional plots)  
40 of all the world ocean  $\delta^{18}\text{O}$  records during that deglaciation, which suggest incorrectly that  
41 little or no deglaciation occurred during the insolation minimum. In the determination of the  
42 amplitude of the  $\delta^{18}\text{O}$  proxy changes, the internal factors within Earth’s climate system are  
43 apparently stronger than the direct effects of insolation variations, such as changes in glacial  
44 melting rates. This is emphatically true for the deglaciation of the Drenthe sub stage of the  
45 Saalian glaciation.

46



1 **3 Why the  $\delta^{18}\text{O}$  proxy record failed: the blockage of Siberian rivers by glacial ice flow**  
2 **3.1 The Eurasian ice sheet and its giant lake**  
3 The largest Eurasian ice sheet of the Pleistocene may have occurred at the  
4 extreme of the Saalian glaciation (Arkhipov et al., 1995), depicted in Figure 2. Glacial ice  
5 covered most of the British Isles and extended without a break across Scandinavia and  
6 western Siberia almost to the Lena River. To the north it covered the shallow Barents  
7 Sea and the Svalbard archipeligo. To the south it reached into the Dniepr River valley not  
8 far from the Black Sea. After a weak interstadial about 170 ka, the falling (less negative)  
9  $\delta^{18}\text{O}$  values in Figure 1 indicate continuing ice sheet growth to point A in Figure 1 at 156  
10 ka. The positive fall of the  $\delta^{18}\text{O}$  then stopped because polar ocean fractionation began, as  
11 discussed in Sect. 5. But Drenthe glacial ice continued to accumulate with profound  
12

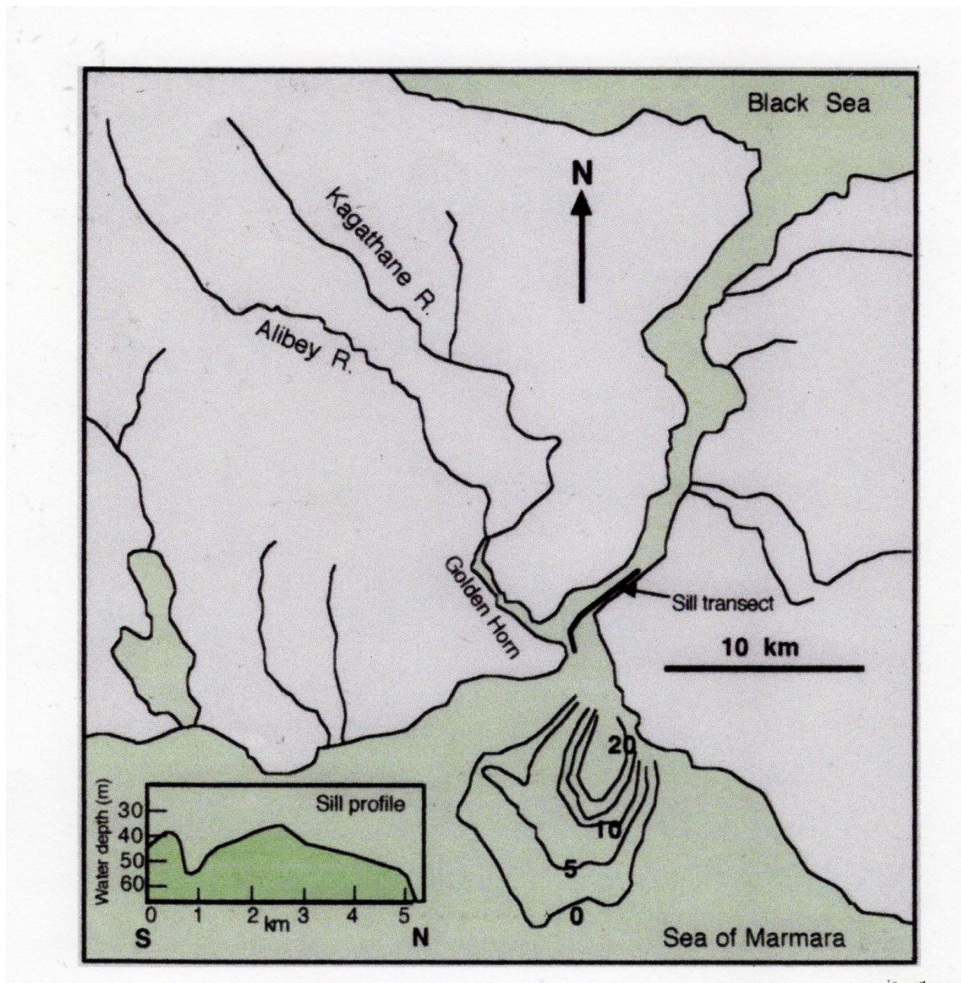


13  
14  
15 **Figure 2 The maximum extent of the Drenthe substage of the Saalian glaciation**  
16 **at 142 ka. Cross-hatched area is the catchment for melt water and precipitation that**  
17 **drained through the Mediterranean Sea to the North Atlantic during the Drenthe**  
18 **deglaciation. Slightly modified from Arkhipov et al. (1995).**

19  
20 consequences, and sea level continued to fall. Beginning probably a little before 155 ka in  
21 the latter part of the Saalian cycle with the Mackenzie River covered by the Canadian ice  
22 sheet of that time, the two largest Siberian rivers, the Ob, the Yenisey, and other smaller  
23 rivers that also discharge into the polar ocean became blocked by glacial ice flow. A third  
24 major Siberian river, the Lena, remained unblocked, but in the dry glacial climate its



1 discharge into the polar ocean would have been small. Consequently the deep polar ocean  
2 was no longer effectively capped and stratified by river water. Sea ice there would have  
3 been largely absent throughout the year because in unstratified deep water vertical  
4 convection would prevent cooling to the freezing point. As the polar ice disappeared, all  
5 the polar changes discussed in Sect. 5 began to occur, while accompanied by the further  
6 buildup of world glacial ice and the rise of the water level of the giant lake in Siberia.  
7



8  
9  
10  
11  
12  
13  
14  
15  
16

**Figure 3** The Bosphorus Strait with sill depth profile. North of the sill transect (heavy dark line) water depths are 90 m-100 m. Minimum bedrock depth at the sill is 65 m below present sea level. Minimum sediment depth is 35 m. The delta profiles are sonar reflection times that depict sediments discharged through the Golden Horn in more pluvial times. Combined from Gunnerson and Özturgut (1974) and Alavi et al. (1989).



1           The catchment area of the ice-blocked Siberian rivers extended 3000 km from the  
2 Ural Mountains to Lake Baikal (Arkhipov et al., 1995). Within that area the ice-blocked  
3 lake began to form. The exact date of the start of the blockage is unknown, but in the dry  
4 glacial climate the lake level slowly rose over thousands of years to a maximum and began  
5 to overflow through the Turgai pass at its present elevation of 121 m (Google Earth). At  
6 that maximum the lake area was about 1,100,00 km<sup>2</sup>, or three times the area of the modern  
7 Caspian Sea.

8           The overflow would have begun as a somewhat abrupt event about 142 ka if, as is  
9 likely, rapid erosion of sediment in the pass occurred. The overflow quickly filled the  
10 basins of the Aral, Caspian, and Black Seas with mixed melt water that flowed onward  
11 through the Bosphorus strait (Fig. 3), through the Mediterranean, and into the North  
12 Atlantic at Gibraltar. In the arid glacial climate before the overflow, the water levels in  
13 those isolated inland seas would have been quite low with limited river inputs.

### 14           **3.2 A pulse of melt water from the Black Sea: the Bosphorus sediment dam**

15           A strong pulse of giant lake melt water into the North Atlantic would have been  
16 enabled by a sediment dam failure at the south end of the Bosphorus. The pulse capped the  
17 high latitude North Atlantic with lower salinity water and initiated deglaciation. A  
18 Holocene sediment dam analog is known. At a calendar age of 9.4 ka (Major et al., 2006) a  
19 rising world sea level at about -20 m washed out a sediment dam on the -65 m bedrock sill  
20 (Fig. 3) and flooded northward into the arid Black Sea basin, with the Black Sea level  
21 initially down at -100 m or more. The ~40 m of sediment on the sill had been deposited  
22 during a high sea level at a more pluvial time like the present when the Bosphorus flow was  
23 mainly out of the Black Sea into the Mediterranean.

24           At high interglacial or interstadial sea levels the Bosphorus flow is a two-way  
25 exchange flow, but as ice sheets grow and the world sea level falls, the flow would become  
26 only outward into the Mediterranean until cut off by the increasingly dry glacial climate in  
27 the Black Sea catchment. During pluvial interglacial times the sediment from the  
28 Kagathane and Alibey Rivers is carried into the strait through the Golden Horn at the south  
29 end of the bedrock sill (Fig. 3). Before the cutoff, the southward flow of the Bosphorus  
30 current over the sill entrains Mediterranean water, which is replaced by a northward bottom  
31 inflow that moves the sediment up onto the sill. The present sediment thickness is about 30  
32 m, and repetitive dams of at least that thickness would be expected after times of previous  
33 cyclic sea level maxima in the Pleistocene. The giant lake overflow and resulting events are  
34 supported by an eastern Mediterranean deep-sea sediment record.

35

## 36           **4 The Mediterranean record of the chain of Late Saalian events that were** 37 **associated with the failure of the world ice volume $\delta^{18}\text{O}$ proxy**

### 38           **4.1 Dating the Mediterranean record of core TR172-22**

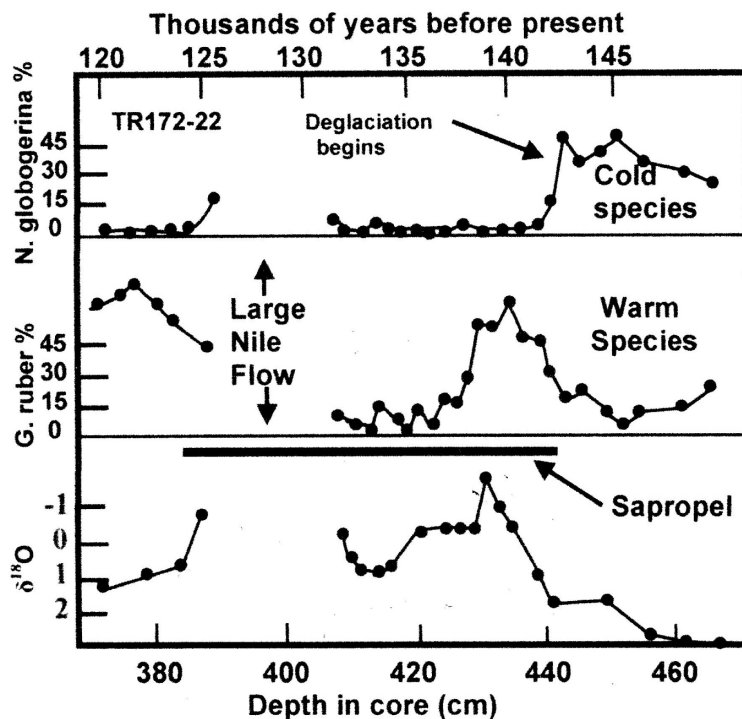
39           Evidence of the giant lake overflow and subsequent events are found in sediments  
40 of eastern Mediterranean core TR172-22 as reported by Thunell and Williams (1982).  
41 This core was recovered from a site half way between Crete and Cyprus. The core data  
42 replotted in Figure 4 are dated by centering the low-salinity interval of absent  
43 foraminiferal data on the accurately calculated 25° N caloric summer insolation  
44 maximum at 128 ka (Berger, 1978) when the strongest monsoons occurred and  
45 Mediterranean salinity was at a minimum. Uniform sedimentation is assumed. Beginning  
46 at 130 ka the swollen Nile River made the eastern Mediterranean surface water too fresh



1 for salt-water foraminifera to survive. The strong monsoons and large Nile flow imply an  
2 absence of summer cooling in northern Africa due to the less extreme extent of the ice  
3 sheets at the end of the Warthe substage of the Saalian, about 130 ka. This contrasts with  
4 the glacial cooling of northern Africa that apparently occurred toward the extreme of the  
5 Drenthe sub stage about 150 ka despite high insolation (Fig. 1). The cooling probably  
6 prevented strong monsoons and any deglacial  $\delta^{18}\text{O}$  proxy response at that time. Such a  
7 strong cooling may have caused a glaciation in the Atlas Mountains of northwestern  
8 Africa (Hughes et al., 2011).

#### 9 4.2 The Mediterranean record: The giant lake overflow

10 At or shortly before 142 ka when world sea level was quite low, the giant Siberian  
11 lake burst through sediment constraints at the Turgai pass, successively flooded the  
12 isolated Aral and Caspian basins, and poured into the Black Sea through the Manytsh  
13 channel (Arkhipov et al., 1995). When the overflow at the Bosphorus began, its sediment  
14 dam (Fig. 3) was abruptly washed out and the Black Sea level would have fallen rapidly



15  
16 **Figure 4** Sedimentary records from core TR172-22 reported by Thunell and  
17 Williams (1982) in the eastern Mediterranean from the beginning of the Drenthe  
18 deglaciation to the end of Termination 2. The maximum strength of African  
19 monsoons and minimum Mediterranean salinity coincides with the astronomically  
20 calculated summer insolation maximum at latitude 25° N. Therefore the time scale is  
21 set with the center of the interval of absent salt water foraminifera and maximum  
22 Nile River flow at 128 ka.  
23



1 by possibly as much as 40 m to the present bedrock sill elevation of -65 m. That event is  
2 dated at 142 ka by melt water stratification that preserved summer warmth in the mixed  
3 surface layer of the Mediterranean. This caused the disappearance of the cold-water  
4 foraminiferal *N. globogerina* (top, Fig. 4), and increased the abundance of the warm  
5 water species, *G. ruber*, (middle, Fig. 4). Before the flooding event the Black Sea could  
6 have had salinity like today's, about 18 ‰. After the mixing that occurred during the  
7 flooding, the Black Sea surface salinity would have been somewhat less, possibly less  
8 than half the Mediterranean salinity. Therefore the stratification in the Mediterranean was  
9 quite effective and would have limited the convective circulation that usually oxidizes  
10 benthic sediments, thus initiating the formation of the black sapropel sediments in the  
11 eastern Mediterranean (Fig. 4).

12 If the Bosphorus sediment on the sill had been only 30 m thick as it is today, the  
13 rapid washing out of the dam would have put a large pulse of mixed low-salinity water  
14 equivalent to a 3.2 m layer of the melt water on the Mediterranean surface. This would  
15 have injected a corresponding pulse of lower salinity surface water into the North  
16 Atlantic at Gibraltar. The outflow pulse apparently capped the high latitude seas with  
17 water of reduced salinity that shut down THC, thus reducing North Atlantic Drift flow  
18 from the Gulf Stream and strengthening the southward return flow of the Gulf Stream in  
19 the eastern North Atlantic.

#### 20 **4.3 The Drenthe deglaciation**

21 The loss of the THC would have initiated a deglaciation in Antarctica as well as  
22 North America and Eurasia. With the lack of North Atlantic thermohaline circulation and  
23 resulting loss of mid level inputs of warmer deep-water to the Southern Ocean, the  
24 seasonal winter sea ice extent around the Antarctic continent would always been at a  
25 maximum (Johnson, 2015b). Therefore circumpolar winter storms, moving perpendicular  
26 to the strongest land-sea temperature gradient, remained more distant from the continent  
27 with a severe reduction in Antarctic continental precipitation. In Europe and Asia, it was  
28 probably another seasonal shift in storm paths that rapidly diminished the Saalian ice  
29 sheet. The perennially colder seas bordering Europe to the west would not have been as  
30 cold as the iceberg-filled seas during Heinrich events, but would still have caused a  
31 significant increase in the land-sea temperature gradients there, due to the reduced North  
32 Atlantic Drift and the resulting more sharply defined colder return flow of the Gulf  
33 Stream off the west coast of Spain. Land temperatures in Western Europe in winter were  
34 likewise cold, and the jet stream that guided winter storms would have been located on a  
35 west-to-east path at the latitude of Spain and well south of the ice, thus preventing the  
36 Eurasian ice sheet from receiving heavy snows. But in summer the jet stream would have  
37 been quite different. With the summer warming of the land masses, the colder sea-warm  
38 land temperature contrasts in France and Spain would have shifted the jet stream to a  
39 southwest-northeast path, and the jet stream flow and the storms that follow it would  
40 have carried warmer and dryer air from as far south as northwestern Africa into the  
41 Eurasian ice sheet region, with a strong deglacial effect.

#### 42 **4.4 A rapid Warthe glaciation terminated by strong monsoons**

43 The Drenthe deglaciation supplied an increasing amount of melt water to the  
44 Mediterranean over several thousand years, as suggested by the increasing abundance of  
45 warm water foraminifera as stratification became more effective and sea surface  
46 temperatures rose (Fig. 4). But when the Siberian rivers again drained into the polar



1 ocean at 136.5 ka, the Turgai pass overflow stopped, and the polar ocean became briefly  
2 stratified. However, as the Warthe glacial sub stage began, glacial growth was renewed  
3 and the Siberian rivers became quickly blocked again by ice (Arkhipov et al., 1995),  
4 although with the shorter duration of the Warthe no overflow of the giant lake occurred.  
5 At the start of the Warthe glaciation the initially low insolation and weak monsoons like  
6 today increased Mediterranean salinity and high latitude THC. Therefore starting with  
7 large residual Northern ice sheets, glacial growth was rapid and sea level fell to about -80  
8 m at 130 ka while summer insolation increased by about 6 % in Northern latitudes. This  
9 sea level fall (D, Fig. 1) was indicated by dated fossil corals from rapidly uplifted New  
10 Guinea as reported by Esat et al. (1999). But strong monsoons began about 130 ka thus  
11 increasing the Nile flow, lowering Mediterranean salinity, eliminating the saltwater  
12 foraminifera (Fig. 4), and lowering the rate and salinity of the Mediterranean outflow.  
13 This reduced the glacial climate THC, altered the storm paths, and initiated the rapid  
14 deglaciation of Termination 2 that ended about 126 ka (E, Fig. 1), paradoxically under  
15 the influence of stronger THC in the northern Greenland Sea basin as argued in the Sect.  
16 6 summary.

17

## 18 **5 Why the oceanic $\delta^{18}\text{O}$ proxy record failed: fractionation in the polar ocean**

19

### 20 **5.1 The cause of the anomalous $\delta^{18}\text{O}$ record of the late Saalian glaciation**

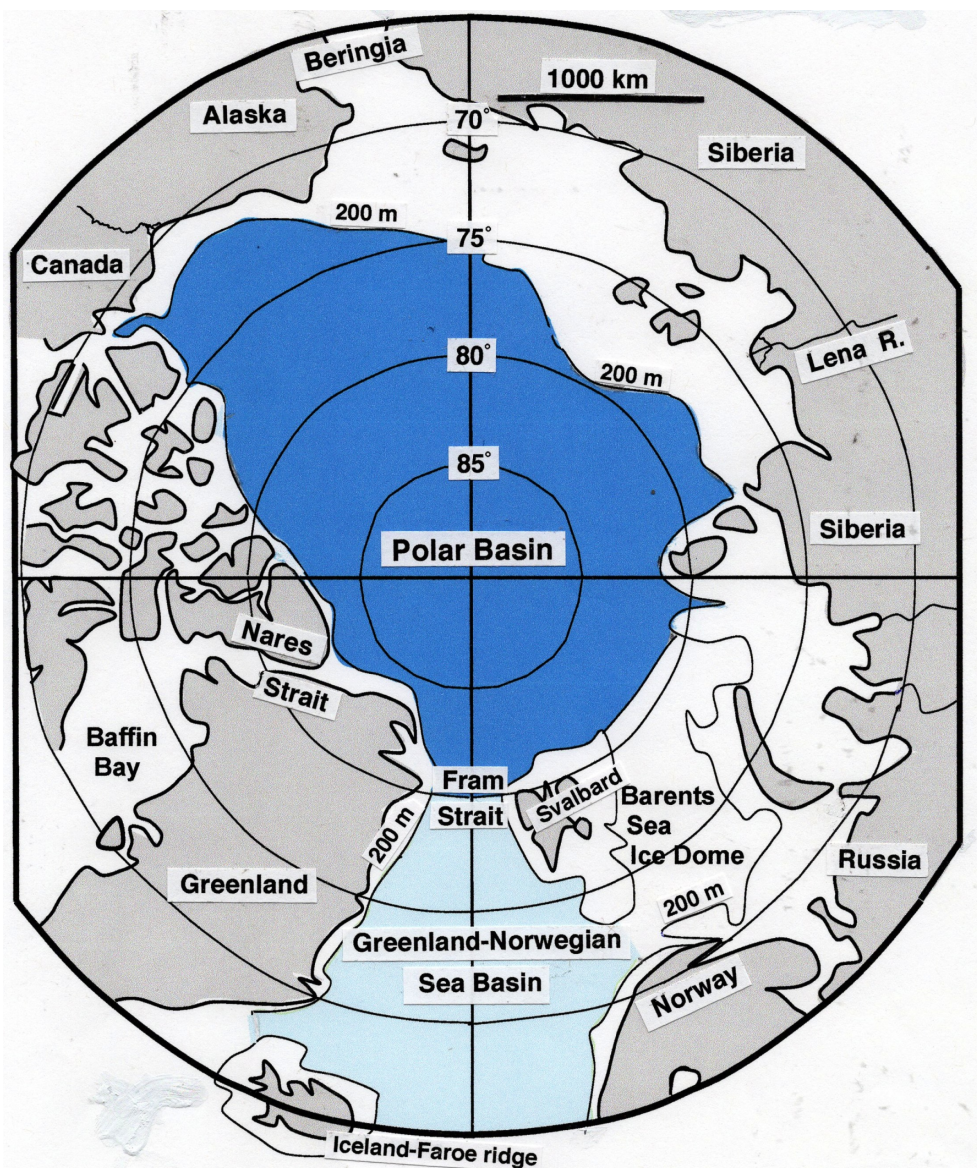
21

22 The  $\delta^{18}\text{O}$  enrichment of the world ocean by evaporative fractionation is the basis  
23 for the  $\delta^{18}\text{O}$  proxy for ice volume and sea level change. World ocean  $\delta^{18}\text{O}$  values change  
24 in a positive direction as glacial ice volume increases. But if an isolated body of water  
25 becomes enriched in  $\text{H}_2^{18}\text{O}$  by fractionation, the world ocean becomes correspondingly  
26 depleted in  $\text{H}_2^{18}\text{O}$ , making the measured oceanic  $\delta^{18}\text{O}$  increasingly negative (too high on  
27 the page in conventional data plots as in Figure 1). Such a negative error might have had  
28 contributions due to fractionation in the isolated Black, Caspian, and Aral seas, or the  
29 giant ice-blocked Siberian lake east of the Ural Mountains. However, these inland seas  
30 receive water from precipitation that is quite deficient in  $\text{H}_2^{18}\text{O}$ , and relative to the world  
31 ocean their surface areas are small. Therefore their contributions to the  $\delta^{18}\text{O}$  errors were  
32 negligible. The Mediterranean Sea with its vigorous exchange currents at Gibraltar  
33 (Bryden and Kinder, 1991) and a present mixing time of about 120 yrs is not sufficiently  
34 isolated.

35

36 On the other hand the polar ocean (Fig. 5) is large enough and isolated enough at  
37 the glacial extreme to have undergone the fractionation and sequestration of  $\text{H}_2^{18}\text{O}$  that  
38 distorted the world  $\delta^{18}\text{O}$  record. It was much more isolated than it is today, with the  
39 Beringia land bridge exposed and the Barents Sea ice dome blocking flow north of  
40 Scandinavia. With lower sea level later in the glacial cycle, the main concern here is the  
41 deeper polar ocean. The deep ocean begins at the edge of the continental shelves, taken  
42 here to be close to a present depth of 200 m. Depths of 4000 m or more are found in parts  
43 of the polar basin. The area with present depths greater than 200 m (Fig. 5) is  $5.1 \times 10^6$   
44  $\text{km}^2$ , twice the area of the Mediterranean Sea or 6.7 million  $\text{km}^2$  when the deep  
45 Greenland-Norwegian basin is included. The polar ocean's connection to the world ocean  
46 was through the 3700 m-deep channel in the Fram Strait into the Greenland-Norwegian  
47 basin, and then over the Iceland-Faroe ridge, a broad plateau with present sill depth of  
48 about 480 m.

49



1  
2  
3  
4  
5  
6  
7  
8  
9  
10  
11

**Figure 5** A sketch map of the North Polar regions using a polar projection to show the deeper parts of the polar ocean basin and the Greenland-Norwegian Sea basin at present depths greater than 200 m. Redrawn from Bartholomew's *Advanced Atlas of Modern Geography*, 1950, McGraw-Hill Inc., New York.

The deep polar ocean area of  $5.1 \times 10^6 \text{ km}^2$  is far less than the world ocean area of  $320 \times 10^6 \text{ km}^2$ . Nevertheless over the long intervals of time similar amounts of fractionation could have occurred. In Figure 1 in the interval A-B an additional world sea level fall of about 50 m probably occurred, which implies that  $16 \times 10^6 \text{ km}^3$  of water were



1 evaporated and precipitated on ice sheets in about 13,000 yrs. The same quantity of polar  
2 ocean water would have been evaporated and carried away during that interval if the  
3 annual rate of evaporative loss was equivalent to a plausible polar ocean layer 22 cm-  
4 thick. From thermodynamic considerations fractionation is more effective for water  
5 evaporated at low polar temperatures than for water evaporated in warmer latitudes.  
6 Consequently, the low polar temperatures would have contributed to the deficit of  $\text{H}_2^{18}\text{O}$   
7 in the world ocean that was slightly larger than the excess caused by additional world ice  
8 accumulation, as suggested by the small negative rise of the  $\delta^{18}\text{O}$  value in Figure 1  
9 between 156 ka and 142 ka.

### 10 **5.2 Circulation in a sea-ice-free polar ocean**

11 The change to an ice-free polar ocean would have caused important polar  
12 circulation differences relative to today. With modern winter sea ice covering the polar  
13 ocean, I observed satellite images in year 2011 posted by the Technical University of  
14 Denmark on the internet that showed sea ice moving roughly clockwise around the pole,  
15 consistent with wind stresses due higher atmospheric pressures over the cold ice. As the  
16 flow approached Greenland it split apart with much of the flow going westward, but a  
17 minor part continued southward along the eastern Greenland coast. The ice-filled East  
18 Greenland Current is therefore now a visible drain on the surface water of the polar basin.  
19 In other times like today, the THC is likewise a drain on the Greenland-Norwegian Sea  
20 basin.

21 However, during the long winters near the Drenthe extreme with an open polar  
22 ocean, the polar atmosphere would have been warmer than that over surrounding cold  
23 lands. The probable result was the generation of large counterclockwise cyclonic storm  
24 systems that were dragged slowly eastward by the effect of Earth's rotation on the bulk of  
25 the each storm area. The storm centers of rotation were probably well off shore, and the  
26 net effect of wind stresses on the sea surface would have driven the oceanic circulation  
27 around the polar basin in a counterclockwise direction. The northward projection of the  
28 Greenland coast in Figure 5 would therefore not have diverted polar water flow into the  
29 East Greenland Current as it does today with clockwise polar flow. If so, the main  
30 transfer through the upper levels of the Fram Strait may have been a slow northward drift  
31 of water from the adjacent Greenland basin to replace the net polar ocean evaporation  
32 losses.

### 33 **5.3 An explanation for the massive Eurasian glacial ice buildup.**

34 Another consequence of an open polar ocean is a chain of circulation effects that  
35 may explain the record-breaking extent of the Eurasian ice sheet during the Saalian  
36 glaciation. Northward flow through the Nares Strait between Greenland and Ellesmere  
37 Island (Fig. 5) into the polar ocean may have been indirectly responsible for steering  
38 winter storms through southern Scandinavia into the heart of the Eurasian ice sheet.  
39 Today's flow through the Nares Strait is driven by atmospheric pressure differences over  
40 the 500 km length of the strait. In the year 2011 and early 2012, I observed movement of  
41 clumps of sea ice in high-resolution satellite images posted by the Technical University  
42 of Denmark. On 134 days when flow direction in the strait could be observed, 71 % of  
43 the flow-days were north-to-south and 29 % were south-to-north. With only three  
44 exceptions, atmospheric pressure differences determined the direction of flow. In 2011  
45 pack ice covered the area between the pole and the Canadian-Greenland northern coasts.  
46 But when that area was free of sea ice in the Later Saalian, the warmer atmosphere and



1 lower polar atmospheric pressure may have ensured a dominant northward flow from  
2 Baffin Bay into the polar ocean, both through the strait and through any open channels in  
3 the Queen Elizabeth islands to the west. Therefore without the southward flow of lower  
4 density polar water entering and stratifying Baffin Bay, strong land-sea temperature  
5 contrasts around the perennially open water in the bay would have generated a powerful  
6 low pressure system over Baffin Bay and the Labrador Sea like the one that initiated the  
7 last ice age at 120 ka (Johnson, 2015a).

8 This Labrador Sea Low would then have prevented the development of the nearby  
9 Iceland Low cyclonic system that provides prevailing wind stresses that would be quite  
10 important for driving saline North Atlantic Drift water northeastward into the Norwegian  
11 Current. Today this transport strongly favors thermohaline warming effects west of  
12 Norway and north of the Iceland-Faroe ridge (Johnson, 2015a). Consequently in the Late  
13 Saalian while the Labrador Sea and polar ocean remained ice-free, Northern Hemisphere  
14 thermohaline circulation was likely reduced, but not eliminated because other deep water  
15 would have been forming in the north end of the unstratified ice-free Baffin Bay. But  
16 without the wind stresses of the Iceland Low system, no deep-water may have formed  
17 north of the Faroes, and sea surface temperatures in the Greenland-Norwegian basin  
18 would have been colder with a more stable atmosphere than today. A large fraction of sub  
19 polar storm paths therefore would have been located slightly to the south of Iceland  
20 where a stronger oceanic temperature gradient would have been guiding the jet stream.  
21 Storm paths could then have extended across northern Europe and southern Scandinavia  
22 between latitudes 55° N and 60° N, and such storms would have carried a supply of water  
23 vapor into the central part of the Eurasian ice sheet, ensuring its growth to the maximum  
24 extent of the Drenthe substage glaciation.

#### 25 **5.4 Isolation of the ice-free polar ocean**

26 Unlike the Mediterranean Sea, the polar ocean had a buffer in the form of the  
27 Greenland-Norwegian Sea basin that lies between the polar and the world oceans. As the  
28 Drenthe glaciation built up to its extreme at 142 ka and the dense fractionated water  
29 accumulated in the polar ocean, the buffer basin would have shared the accumulation,  
30 and minimized the release of the dense water to the world ocean. Unlike the Strait of  
31 Gibraltar with its depth of 285 m, no sharp density gradients would likely have been  
32 present within the Fram Strait (Fig. 5) with its maximum depth of 3700 m. Densities on  
33 both sides of the strait would have been similar, and a rapid exchange of water masses  
34 would not have occurred with the counterclockwise polar circulation. With open water  
35 over the deep polar ocean and no insulating pack ice, a lower level polar atmosphere that  
36 was warmer in winter than today is implied. As argued in Sect. 5.2, the temperature  
37 contrast between the warmer atmosphere over the open ocean and the adjacent colder  
38 lands would have generated frequent eastward-moving storm systems with heavy  
39 precipitation over adjacent high Arctic lands. Evidence for such storms is found on the  
40 northern tip of Greenland in Peary Land and on Ellesmere Island to the west. On  
41 Ellesmere and on Peary Land (Fig. 6) much of the land is barren and ice-free because  
42 precipitation rates today are quite low. But the coasts are deeply indented by old fiords  
43 formed by ice streams flowing into the sea. U-shaped valleys are abundant, indicating  
44 that thick ice sheets had covered the land and were fed by precipitation from storms  
45 passing by on the open polar ocean.



1  
2 **Figure 6** Google Earth image of Peary Land on the northern tip of Greenland.  
3 **Image width is about 250 km.**  
4

5 The maximum storm turbulence would have occurred in zones not far from the  
6 coasts where the largest temperature contrasts would have been found. There evaporation  
7 and fractionation rates would have been high causing the sea surface salinity to increase.  
8 The resulting denser and saltier water would tend to sink into the deepest areas and be  
9 replaced by water upwelling from outside the zone. The sinking water would tend to  
10 slowly fill the polar basin with saltier water enriched in  $\text{H}_2^{18}\text{O}$ . The deepest water  
11 enriched in  $\text{H}_2^{18}\text{O}$  would also accumulate in the Greenland-Norwegian basin by  
12 fractionation and by slow deep drift from the polar ocean southward through the Fram  
13 strait. The salinities and concentrations of  $\text{H}_2^{18}\text{O}$  in the two basins at levels below the  
14 present ~480 m-depth of the Iceland-Faroe ridge might not have been greatly different.  
15 The net loss by evaporation in the polar ocean would have been replaced by a slow drift  
16 of less dense water from the Greenland basin through the Fram Strait at higher levels.  
17 Eventually a state of equilibrium circulation would prevail. The depths of the polar ocean  
18 and the Greenland-Norwegian basin below the Iceland-Faroe ridge would continue to fill  
19 with denser and saltier water enriched in  $\text{H}_2^{18}\text{O}$ . Evaporation losses from both basins  
20 would be replaced by slow net flow over the Faroe ridge. The enrichment of polar water  
21 in  $\text{H}_2^{18}\text{O}$  would have been mirrored by depletion in the world oceans, and at the Drenthe  
22 glacial extreme at 142 ka the measured world ocean  $\delta^{18}\text{O}$  could not have reflected the  
23 true low sea level that is suggested by the red dashed line at **B** in Figure 1.  
24

25 **6 Summary of proposed sea level corrections to the Saalian oceanic  $\delta^{18}\text{O}$  record in**  
26 **Figure 1**

27 **6.1 A-B, 156 ka-142 ka**



1 Beginning at **A**, the rate of fractionation and sequestration of  $\text{H}_2^{18}\text{O}$  in the polar  
2 ocean slightly exceeded the rate in the world ocean due to the continuing accumulation of  
3 Drenthe glacial ice. The sea level fall ended at an extrapolated level of -140 m and an age  
4 of 142 ka.

### 5 **6.2 B-C, 142 ka-136.5 ka**

6 The giant lake overflow by way of the Mediterranean Sea capped the northeastern  
7 North Atlantic and stopped Northern THC. This initiated world deglaciation by starving  
8 the ice sheets of moisture. The loss of all Northern THC also caused the loss of Antarctic  
9 thermohaline circulation because, without the THC and warmer Northern intermediate-  
10 level water input, the shelf ice and heavy sea ice expands out over deep water where  
11 convection prevents the seasonal freezing that otherwise results in deep water formation  
12 (Johnson, 2015b). Therefore with the loss of the two main sources of deep water  
13 formation the world ocean became more stratified, and instead of the modern world  
14 ocean mixing time of about a thousand years, the mixing time increased to many  
15 thousands of years. The depressed  $\delta^{18}\text{O}$  at 136.5 ka in Figure 1 might be explained if a  
16 modest THC was restored quite late in the deglaciation before much world mixing had  
17 occurred. Most of the melt water would still have been found in the upper levels of the  
18 ocean. The formerly sequestered  $\text{H}_2^{18}\text{O}$  would have been even more concentrated near  
19 the surface where it would have had little or no effect on the benthic record at that time.  
20 The mixing delay could therefore explain the small rise in  $\delta^{18}\text{O}$  in the V28-238 record  
21 from 142 ka to 136.5 ka. The larger concentration of  $\text{H}_2^{18}\text{O}$  near the ocean surface and  
22 the cold temperatures associated with the incomplete Northern deglaciation would  
23 explain the even greater suppression of  $\delta^{18}\text{O}$  found in typical planktonic sediment  
24 records, making the Drenthe deglaciation almost invisible in both surface and benthic  
25  $\delta^{18}\text{O}$  records.

### 26 **6.3 C-D, 136.5 ka-130 ka**

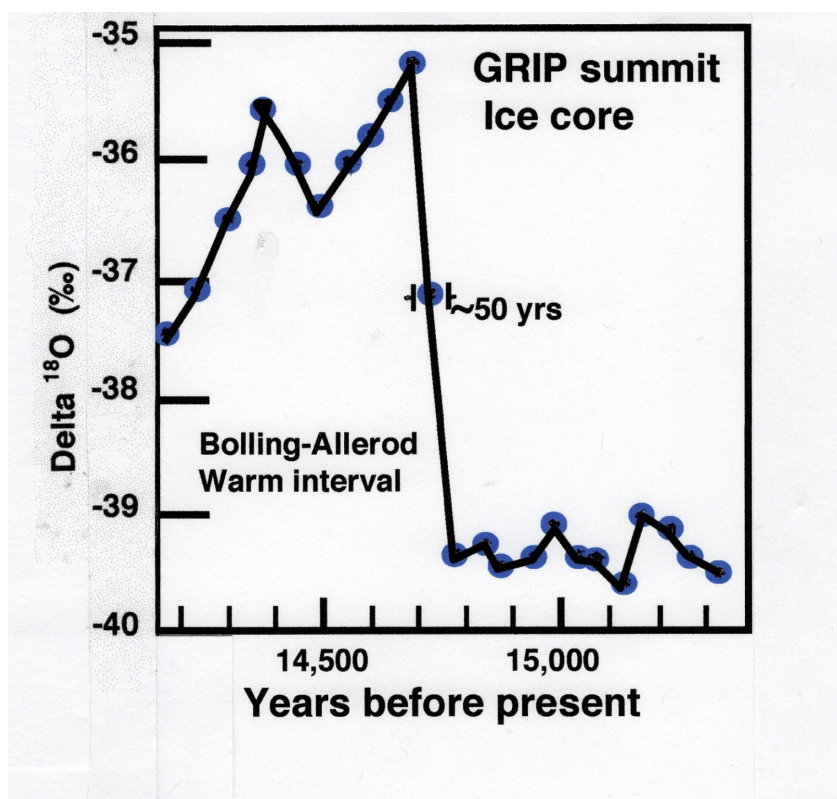
27 Most of the following Warthe glaciation occurred under renewed fractionation in  
28 the polar ocean because the Siberian rivers again became ice-blocked. The Warthe sea  
29 level fell to about -80 m as implied by the shallow-water corals that had grown in  
30 Aladdin's Cave on presently uplifted New Guinea (Esat et al., 1999). Therefore,  
31 somewhat as in the **A-B** interval, the sequestration of  $\text{H}_2^{18}\text{O}$  during the shorter Warthe  
32 interval raised the inferred sea level at **G** to about 30 m above the likely true level.

### 33 **6.4 D-E, 130 ka-126 ka**

34 The end point sea level of this interval at **E** in Figure 1 at the beginning of the last  
35 interglacial was several meters above present (Bender et al., 1979; Chen et al., 1991),  
36 which is roughly consistent with the total  $\delta^{18}\text{O}$  change. However, the details of the  
37 physical changes in the interval **D-E** like those in **B-C** are less clear. The Warthe  
38 deglaciation began when strong African monsoons shut down the THC with low salinity  
39 Mediterranean water, but the interval ended with Northern glacial ice gone and all the  
40 sequestered  $\text{H}_2^{18}\text{O}$  well mixed into the world ocean, implying strong THC. There is a  
41 precedent for such a switch to strong THC early in the last deglaciation. Bond et al.  
42 (1993) reported an abrupt positive jump of almost 5 ‰ in the  $\delta^{18}\text{O}$  of the Greenland  
43 GRIP ice core at 14,700 calendar years before present (Fig. 7). Sea level then, as  
44 measured at the Barbados site, was still low at about -100 m (Figure 2 in Fairbanks,  
45 1989). At about that time an abrupt sea level rise of 30 m began that could only have



1 been caused by a massive loss of Antarctic ice. The  $\delta^{18}\text{O}$  change in the GRIP ice core  
2 was probably caused by the restoration of strong North Atlantic THC.  
3 However, with the linkage of the deep ocean oscillation (Johnson, 2015b), it is  
4 difficult to say if a collapse of Antarctic ice mass was the cause or the effect of the  
5 restored northern THC, although the former seems more likely. A collapse of Antarctic  
6 marine-based ice would have to have occurred early in the Warthe deglaciation to have  
7 produced the complete mixing result, whereas in the Drenthe deglaciation a similar  
8 collapse must have occurred late in the deglaciation before world ocean mixing became  
9 very significant.  
10



11  
12 **Figure 7** A large step change in the  $\delta^{18}\text{O}$  record of a Greenland ice core,  
13 interpreted as the result of the sudden restoration of strong thermohaline  
14 circulation in the Greenland-Norwegian Sea early in the last deglaciation. Modified  
15 from Bond et al. (1993).

## 16 17 7 Discussion and conclusions

### 18 7.1 The rapidity of the Warthe deglaciation: The ice-free Baffin Bay model

19 The sea level fall from +4 m to almost -80 m between 136.5 ka and 130 ka was  
20 remarkably rapid. A factor that favored the rapid fall was the residual ice in Eurasia and  
21 in Canada that remained when the giant Siberian lake was drained away and low-salinity  
22 oceanic capping ceased. But to explain the sea level fall of about 80 m in 6,500 yrs, a



1 mechanism is needed that favors glacial accumulation on both Northern continents and  
2 on the Antarctic continent. The ice-free Baffin Bay scheme proposed for rapid ice  
3 accumulation at the initiation of the last ice age at 120 ka (Johnson, 2015a) would  
4 accomplish this if slightly warmer deep-water formation could be maintained in Baffin  
5 Bay.

6 In the conceptual model for initiation of the last ice age as argued in Sect. 5, a  
7 persistent storm system developed over the warmer and perennially open water in the  
8 Labrador Sea and Baffin Bay, caused by loss of stratification in Baffin Bay at 120 ka.  
9 Strong evidence has been reported (Koerner et al., 1988) for open water at the north end  
10 of Baffin Bay when the last ice age began. They found willow pollen at the base of a core  
11 from Devon Island ice cap in a region where no willows grow today. This observation is  
12 consistent with the report by Fillon (1985) of warmer water foraminifera in deep-sea  
13 sediment at the start of the last ice age in core HU75-58 located 200 km east of the  
14 southern tip of Baffin Island where only polar water species are found today. These  
15 observations imply a persistent cyclonic storm system centered over the Labrador Sea,  
16 which brought an order of magnitude increase in snowfall to northern Canada and  
17 Greenland (Johnson, 2015a). The strength of this cyclonic system also probably  
18 prevented the development of the adjacent Iceland Low pressure system, which  
19 consequently cooled Scandinavia and northern Europe and caused a southward shift of  
20 the stronger oceanic temperature gradients. Storms were then steered over the frozen  
21 Barents Sea and the Scandinavian ice sheet nucleation areas. The open water in the  
22 Labrador Sea west of Greenland was maintained for ~500 yrs, during which world sea  
23 level fell by 2.4 m as measured on uplifted Barbados (Johnson, 2001; Johnson 2015a;  
24 Johnson 2015b). The open water in the Labrador Sea and Baffin Bay was maintained by a  
25 strong and saline West Greenland Current flow that enabled deep water formation to the  
26 north in Baffin Bay despite fresh water input to the Labrador Sea from the Hudson Strait  
27 outflow. The low salinity of that outflow was temporarily counteracted by a more saline  
28 Irminger Current input into the West Greenland Current that was weakened or lost after  
29 ~500 yrs because the deep ocean oscillation (Johnson, 2015b) reduced the Northern THC.

30 In the context of the Warthe glaciation, the deep water formed in the northern part  
31 of ice-free Baffin Bay would have reached the Southern Ocean and limited the formation  
32 of sea ice and shelf ice, thus allowing the circumpolar storm paths to remain close to the  
33 coast to increase the accumulation rate of glacial ice on the Antarctic continent. However,  
34 to make this concept work continuously for the ~6,000 yr-long Warthe glaciation, during  
35 which the Irminger current would often have been weak, the Hudson Strait fresh water  
36 outflow that lowers Labrador Sea salinity must have been blocked from the start of the  
37 new Canadian glaciation to ensure the higher salinity needed for deep-water formation in  
38 Baffin Bay. There is a recent analog for the blockage of Hudson Strait late in the last  
39 deglaciation when the North American ice sheet had become much smaller. At 10.9 ka  
40 (calendar years) a re-advance of the Laurentide ice sheet across Ungava Bay extended as  
41 far to the north as the Hall Peninsula and completely blocked Hudson Strait (Stravers et  
42 al, 1992). Blockage of Hudson Strait after several thousand years of early ice sheet  
43 growth is also suggested by the model of Andrews and Mahaffy (1976). A similar lasting  
44 blockage of Hudson Strait may have facilitated an ice-free Labrador Sea and the Warthe  
45 glaciation. Blockage may have also triggered the renewed glaciation at about 200 ka and  
46 the subsequent ~55 m fall of sea level that ended about 193 ka (Fig. 1). Therefore an ice-



1 blocked Hudson Strait and an ice-free Labrador Sea and Baffin Bay may have  
2 occasionally initiated long intervals of uninterrupted ice sheet accumulation and rapid  
3 world sea level fall during the Pleistocene.

#### 4 **7.2 Conclusions**

5 The consequences of fractionation and sequestration of  $\text{H}_2^{18}\text{O}$  in the ice-free polar  
6 ocean remove much of the confusion associated with evidence for events that occurred in  
7 the world climate records during Termination 2. The root cause of the fractionation was  
8 the extreme extent of Eurasian glacial ice that blocked Siberian river flow into the polar  
9 ocean, and this is consistent with the concept that the moisture supply is the dominant  
10 factor in the growth or shrinkage of glacial ice sheets. During the Pleistocene, the  
11 Mediterranean salinity and strong African monsoons that are controlled by orbital  
12 precession may play a decisive role in reducing the moisture supply and ensuring the  
13 nearly complete removal of Northern Hemisphere glacial ice.

#### 14 **Acknowledgment**

15 This paper is dedicated to the memory of Herbert E. Wright, Jr. (1917-2015).  
16 Without his generous support and his many friendships in the European paleoclimate  
17 community, this paper would not have been written.

#### 18 **References**

- 19  
20  
21 [1] Arkhipov, S.A., J. Ehlers, R.G. Johnson, and H.E. Wright, 1995, Glacial drainage  
22 towards the Mediterranean during Middle and Late Pleistocene: *Boreas*, v. 24, p.  
23 196-206.
- 24 [2] Milankovitch, M., 1930, *Mathematische Klimalehre un astronomische theorie der*  
25 *klimaschwankungen: in Handbuch der Klimatologie*, T.A. Gebruder, ed.  
26 Borntraeger, Berlin.
- 27 [3] Hodell, D.A., 2016, The smoking gun of the ice ages: *Science*, v. 354, p. 1235-1236.
- 28 [4] Hays, J.D., J. Imbrie, and N.J. Shackleton, 1976, Variations in the Earth's orbit:  
29 Pacemaker of the Ice Ages: *Science*, v. 194, p. 1121-1132.
- 30 [5] Johnson, R.G., 2001, Last interglacial sea stands on Barbados and an early anomalous  
31 deglaciation timed by differential uplift: *J. Geophys. Res.*, v. 106, no. C6, p.  
32 11543-11551.
- 33 [6] Wunsch, C., 2004, Quantitative estimate of the Milankovitch-forced contribution to  
34 observed Quaternary climate change: *Quat. Science Rev.*, v. 23, p. 1001-1012.
- 35 [7] Berger, A.L., 1978, Long-term variations of caloric summer insolation resulting from  
36 the Earth's orbital elements: *Quat. Res.*, v. 9, p. 139-167. Tabulated data  
37 supplied by personal communication.
- 38 [8] Rossignol-Strick, M., 1983, African monsoons: an immediate response to orbital  
39 insolation: *Nature*. v. 304. p. 46-49.
- 40 [9] Rossignol-Strick, M., Paterne, M., Bassinot, F.C., Emeis, K.-C., and De Lange, G.J.,  
41 1998, An unusual mid-Pleistocene monsoon period over Africa and Asia: *Nature*,  
42 v. 392, p. 269-272.
- 43 [10] Chappell, J., 1974, Geology of coral terraces, Huon Peninsula, New Guinea: a study  
44 of Quaternary tectonic movements and sea-level changes: *Geol. Soc. Am. Bull.*  
45 v. 85, p. 553-570.
- 46 [11] Stirling, C.H., T.M. Esat, K. Lambeck, and M.T. McCulloch, 1995, High precision U-



- 1 series dating of corals from Western Australia and implications for the timing and  
2 duration of the last interglacial: *Earth Planet. Sci. Lett.*, v. 135, p. 115-130.
- 3 [12] Johnson, R.G., 2015a, Initiation of the last ice age in Canada by extreme  
4 precipitation resulting from a cascade of oceanic salinity increases: *J. of*  
5 *Advances in Natural Sciences*, v. 3, p. 237-251.
- 6 [13] Johnson, R.G., 2015b, Did a bi-polar multi-level oceanic oscillation cause the Little  
7 Ice Age and other high latitude climate extremes? *J. of Advances in Natural*  
8 *Sciences*, v. 3, p. 228-236.
- 9 [14] Lamb, H.H., 1995, *Climate History and the Modern World: second edition*, Routledge,  
10 London: p. 60.
- 11 [15] Lamb, H.H., 1972, *CLIMATE: Present, Past, and Future: v. 1*, Methuen and  
12 Company, p. 338.
- 13 [16] Bryden, H.L., and T.H. Kinder, 1991, Steady two-layer exchange through the Strait of  
14 Gibraltar: *Deep-Sea Res.*, v. 38, p. 5445-5463.
- 15 [17] Ruddiman, W.F. and A. McIntyre, 1979, Warmth of subpolar North Atlantic Ocean  
16 during Northern Hemisphere ice-sheet growth: *Science*, v. 204, p. 173-175.
- 17 [18] Johnson, R.G., and S.-E. Lauritzen, 1995, Hudson Bay-Hudson Strait jokulhlaups and  
18 Heinrich events: a hypothesis: *Palaeogeog., Palaeoclimat., Palaeoecol.*, v. 117, p.  
19 123-137.
- 20 [19] Heinrich, H., 1988, Origin and consequences of cyclic rafting in the Northeast  
21 Atlantic Ocean during the past 130,000 years: *Quat. Res.*, v. 29, p. 143-152.
- 22 [20] Shackleton, N.J., and N.D. Opdyke, 1973, Oxygen isotope and paleomagnetic  
23 stratigraphy of equatorial Pacific core V28-238: Oxygen isotope temperatures  
24 and ice volumes on a  $10^5$  and  $10^6$  year scale: *Quat. Res.*, v. 3, p. 39-55.
- 25 [21] Johnson, R.G., 1982, Brunhes-Matuyama magnetic reversal dated at 790,000 yr B.P.  
26 by marine-astronomical correlations: *Quat. Res.*, v. 17, p. 135-147.
- 27 [22] Major, C.O., S.L. Goldstein, W.B.F. Ryan, G. Lericolais, A.M. Piotrowski, and I.  
28 Hajdas, 2006, The co-evolution of Black Sea level and composition through the  
29 last deglaciation and its paleoclimatic significance: *Quat. Sci. Rev.*, v. 25, p.  
30 2031-2047.
- 31 [23] Gunnerson, C.G., and E. Özturgut, 1974, The Bosphorus: in *The Black Sea –*  
32 *Geology, Chemistry, and Biology*, AAPG Memoir #20, p. 99-114.
- 33 [24] Alavi, S.N., M. Okyar, and K. Timur, 1989, Late Quaternary sedimentation in the  
34 Strait of Bosphorus: High-resolution seismic profiling: *Marine Geology*, v. 89, p.  
35 185-205.
- 36 [25] Thunell, R.C., and D.F. Williams, 1982, Paleoceanographic events associated with  
37 termination II in the eastern Mediterranean: *Oceanologica Acta*, v. 5, p. 229-233.
- 38 [26] Hughes, P.D., C.R. Fenton, and P.L. Gibbard, 2011, Quaternary Glaciations of the  
39 Atlas Mountains, North Africa: in *Quaternary Glaciations-Extent and*  
40 *Chronology*, J. Ehlers, P.D. Gibbard and P.D. Hughes, eds. In: *Dev. in Quat.*  
41 *Sci.*, v. 15, p. 1065-1074.
- 42 [27] Esat, T.M., M.T. McCulloch, J. Chappell, B. Pillans, and A. Omura, 1999, Rapid  
43 fluctuations in sea level recorded at Huon Peninsula during the penultimate  
44 deglaciation: *Science*, v. 238, p. 197-201.
- 45 [28] Bender, M.L., R.G. Fairbanks, F.W. Taylor, R.K. Mathews, J.G. Goddard, and W.S.



- 1 Broecker, 1979, Uranium-series dating of the Pleistocene reef tracts of Barbados  
2 West Indies: Geological Soc. Am. Bull. 90, p. 577-594.
- 3 [29] Chen, J.H., H.A. Curran, B. White, and G.J. Wasserburg, 1991, Precise chronology of  
4 the last interglacial period:  $^{234}\text{U}$ - $^{230}\text{Th}$  data from fossil coral reefs in the  
5 Bahamas: Geological Soc. Am. Bull. 103, p. 82-97.
- 6 [30] Bond, G., W. Broecker, S. Johnsen J. McManus, L. Labeyrie, J. Jouzel, and G.  
7 Bonani, 1993, Correlations between climate records from North Atlantic sediments  
8 and Greenland ice: Nature, v. 365, p. 143-147.
- 9 [31] Fairbanks, R.G., 1989, The age and origin of the “Younger Dryas climate event” in  
10 Greenland ice cores: Paleooceanography, v.5, p. 937-948.
- 11 [32] Koerner, R.M., J.C. Bourgeois, and D.A. Fischer, 1988, Pollen analysis and  
12 discussion of time-scales in Canadian ice cores: Ann. Glaciol. v. 110, p. 85-91.
- 13 [33] Fillon, R.H., 1985, Northwest Labrador Sea stratigraphy, sand input and  
14 paleooceanography during the last 150,000 years: in Andrews, J.T., ed.,  
15 Quaternary Environments: Eastern Canadian Arctic, Baffin Bay and Western  
16 Greenland, Boston: Allen and Unwin, p. 210-247.
- 17 [34] Stravers, J.A., G.H. Miller, and D.S. Kaufman, 1992, Late glacial ice margins and  
18 deglacial chronology for southeastern Baffin Island and Hudson Strait, eastern  
19 Canadian Arctic: Can. J. of Earth Science, v. 29, p. 1000-1017.
- 20 [35] Andrews, J.T., and M.A.W. Mahaffy, 1976, Growth rate of the Laurentide Ice Sheet  
21 and sea level lowering with emphasis on the 115,000 BP sea level low: Quat.  
22 Res. v. 6, p. 167-183.
- 23